Journal of Alloys and Compounds 525 (2012) 126–132

Contents lists available at SciVerse ScienceDirect

Journal of Alloys and Compounds

journal homepage: www.elsevier.com/locate/jallcom

Synergistic hydrogen desorption behavior of magnesium aluminum hydride synthesized by mechano-chemical activation method

Cheng-Hsien Yang, Tzu-Teng Chen, Wen-Ta Tsai*

Department of Materials Science and Engineering, National Cheng Kung University, Tainan 701, Taiwan

ARTICLE INFO

Article history:
Received 23 December 2011
Received in revised form 7 February 2012
Accepted 9 February 2012
Available online xxx

Keywords:
Magnesium aluminum hydride
Mechano-chemical activation synthesis
Dehydrogenation reaction
In situ synchrotron X-ray diffraction

ABSTRACT

A mechano-chemical activation synthesis (MCAS) is employed to fabricate $Mg(AlH_4)_2$ via milling the precursors, specifically $NaAlH_4$ and $MgCl_2$. The corresponding dehydrogenation behavior of the synthesized powders is investigated. The experimental results showed that incomplete synthesis or premature dehydrogenation may occur if the milling process was not properly controlled. The hydrogen content of each synthesized powder is determined by using a thermal gravimetric analyzer (TGA). The dehydrogenation reactions of the synthesized powders are investigated by employing ex situ X-ray diffraction (XRD), in situ synchrotron XRD and differential thermal analysis (DTA). The results showed that the incompletely synthesized powder consisted of residual $NaAlH_4$ in the synthesized $Mg(AlH_4)_2$, which demonstrated an initial dehydrogenation temperature as low as 100 °C and accompanied with a maximum amount (3.1 wt%) of H_2 released below 350 °C. The mutual catalytic effect of both $NaAlH_4$ and $Mg(AlH_4)_2$ on lowering their initial dehydrogenation temperature is confirmed.

1. Introduction

Recently, complex metal hydride systems have become a group of promising hydrogen carriers because of their satisfactory hydrogen density and medium hydrogen release temperature [1–4]. Typical complex metal hydrides considered for the hydrogen storage consist of amides, imides, metal borohydrides, and metal aluminum hydrides (commonly known as metal alanate), etc. For the commercial metal aluminum hydrides such as $LiAlH_4$ and $NaAlH_4$, their theoretical gravimetric hydrogen density and first step dehydrogenation temperature are 10.5 wt%/127–165 °C and 7.4 wt%/229–247 °C, respectively [1,5]. Obviously, their dehydrogenation temperature is not low enough for practical PEM-fuel cell applications on vehicles, even with the utilization of heat from the operating fuel cell (70–110 °C) to facilitate the hydrogen liberation [6].

To lower the dehydrogenation temperature, modification of complex metal hydride by metal cation substitution is a possible approach. Nakamori et al. [7–9] indicated that charge transfer from M^{n+} (partial group IA, IIA, and transition metal) to $[BH_4]^-$ is a substantial feature for the stability of $M(BH_4)_n$, which can be estimated by Pauling electronegativity (χ_P) of M. The degree of charge transfer becomes smaller with increasing value of χ_P, which makes ionic bond weaker. As a result, the unstable hydrides release hydrogen at lower temperature. Based on this correlation between χ_P of M and the dehydrogenation temperature, magnesium aluminum hydride, $Mg(AlH_4)_2$, is considered to be one of the potential materials for hydrogen storage.

Since its first synthesis in 1950 by Wiberg and Bauer [10], several methods had been developed for the fabrication of $Mg(AlH_4)_2$. Metathesis of $NaAlH_4$ and $MgCl_2$ in diethyl ether (Et_2O) or tetrahydrofuran (THF) solvent according to reaction (1)

$$2NaAlH_4 + MgCl_2 + Et_2O/THF \rightarrow Mg(AlH_4)_2{\cdot}Et_2O/THF + 2NaCl(in Et_2O/THF) \quad (1)$$

followed by extraction and purification according to reaction (2)

$$Mg(AlH_4)_2{\cdot}Et_2O/THF \rightarrow Mg(AlH_4)_2 + Et_2O/THF \quad (2)$$

were reported by Fichtner et al. [11–14]. Mechano-chemical activation synthesis (MCAS) by a dry ball milling process via reaction (3), namely

$$2NaAlH_4 + MgCl_2 \rightarrow Mg(AlH_4)_2 + 2NaCl \quad (3)$$

was also reported recently [15–19].

The thermal dehydrogenation behavior of the $Mg(AlH_4)_2$ had also been explored. Claudy et al. [20] proposed that the first step dehydrogenation of the solvate-free $Mg(AlH_4)_2$ initiates at 130 °C, while the second one happens at about 300 °C. Mamatha et al. [17,18] indicated the dehydrogenation reactions of $Mg(AlH_4)_2$ proceed sequentially in accordance with the following reactions

* Corresponding author at: No.1, University Road, Tainan City 701, Taiwan. Tel.: +886 62757575x62927; fax: +886 62754395.
E-mail address: wttsai@mail.ncku.edu.tw (W.-T. Tsai).

0925-8388/$ – see front matter © 2012 Elsevier B.V. All rights reserved.
doi:10.1016/j.jallcom.2012.02.066

(4) and (5), which had been confirmed by different researchers [12,16,19].

$$Mg(AlH_4)_2 \rightarrow MgH_2 + 2Al + 3H_2 \quad (4)$$

$$MgH_2 + 2Al \rightarrow 0.5Mg_2Al_3 + 0.5Al + H_2 \quad (5)$$

Later, Varin et al. [16] found that prolonged milling caused partial dehydrogenation of the synthesized $Mg(AlH_4)_2$ based on their XRD analyses. However, the study was scarce concerning the effect of synthesis condition on hydrogen desorption behavior, especially for short milling time. In this study, MCAS was applied to prepare $Mg(AlH_4)_2$ via metal cation substitution from $NaAlH_4$. By altering the milling time in a relatively wide range as compared with the study done by Varin et al. [16], the effect of synthesis energy on the constitutions of the synthesized powders was explored, and their corresponding dehydrogenation properties and behaviors were investigated as well. The optimum hydrogen desorption performance, such as the highest hydrogen release amount and the lowest dehydrogenation temperature, was presented.

2. Experimental

2.1. Mechano-chemical activation synthesis of magnesium aluminum hydride

Magnesium aluminum hydride ($Mg(AlH_4)_2$) was synthesized using sodium aluminum hydride ($NaAlH_4$, Sigma–Aldrich, 90% purity) and anhydrous magnesium chloride ($MgCl_2$, Sigma–Aldrich, ≥98% purity) as precursors. The precursors were preserved in a N_2-purified glove box, where both the moisture and the oxygen concentrations were maintained below 1 ppm. In each metathesis batch, 1 g of mixed $NaAlH_4$ and $MgCl_2$ powders with a molar ratio of 2:1 was loaded in a 55-ml cylindrical vessel made of stainless steel. Specific stainless steel balls were also loaded into this vessel before sealing tightly. The ball-to-powder weight ratio was 35:1. Mechano-chemical activation synthesis of $Mg(AlH_4)_2$ was performed using a high energy ball-milling machine (SPEX 8000) for various time, specifically 0.1, 0.5, 1, 2, 5 and 10 h. For the milling time longer than 1 h, milling was executed successively for 30 min followed by a rest for 15 min.

2.2. Materials characterization of the synthesized magnesium aluminum hydride

An X-ray diffractometer (XRD, Rigaku MiniFlex II, Cu K_α radiation) was employed to identify the crystal structure of the various synthesized powders, before and after dehydrogenation. In situ powder X-ray diffraction (in situ XRD) was also performed with the aid of Synchrotron Radiation Facility (beamline 01C2 in National Synchrotron Radiation Research Center in Hsinchu, Taiwan). In each analysis, the synthesized powder was loaded in a 1-mm diameter glass capillary tube, and then mounted to the specimen holder. One end of the tube was introduced with a dynamic N_2 gas flow and the other end was open to the atmosphere. During diffraction analysis, the sample was uniformly heated from room temperature to 365 °C at a ramping rate of 5 °C min^{-1} by blowing hot air outside the capillary tube. The wavelength of the synchrotron X-ray was 1.033209 Å. Every 2-D diffraction pattern was successively collected by a Mar345 imaging plate. Then, the 2-D diffraction pattern was converted to 1-D pattern by the Fit2D software. Accordingly, the high temperature transition of crystal structure of the synthesized powders was realized. Besides, the morphology of the synthesized powders was examined using a scanning electron microscope (SEM, Hitachi SU-1500). Elements distribution was characterized using the energy dispersive spectrometer (EDS) equipped on SEM.

2.3. Thermal decomposition and dehydrogenation performance

Differential thermal analyses (DTA) of the milled powders were performed using a NETZSCH STA 409 PC analyzer. In each test, 80 mg of the synthesized powder was loaded in an alumina crucible. The measurement was conducted in an argon gas flow at a rate of 70 ml min^{-1}, and sample heating from room temperature to 350 °C at a rate of 5 °C min^{-1}.

Thermogravimetric analysis (TGA) using a high-pressure microbalance (Cahn D-110) was conducted to evaluate the dehydrogenation behavior of the synthesized powders. The amount of H_2 release and the dehydrogenation temperature were of particular interest. In each test, the synthesized powder with an initial weight of ca. 500 mg was loaded in a quartz crucible and transferred into the high-pressure microbalance chamber. Then, the chamber was evacuated to 1×10^{-4} torr followed by the introduction of H_2 gas (99.999% purity) to ambient pressure. Until the microbalance system was stable, the TGA test from room temperature to 350 °C at a heating rate of 4–5 °C min^{-1} was executed and recorded.

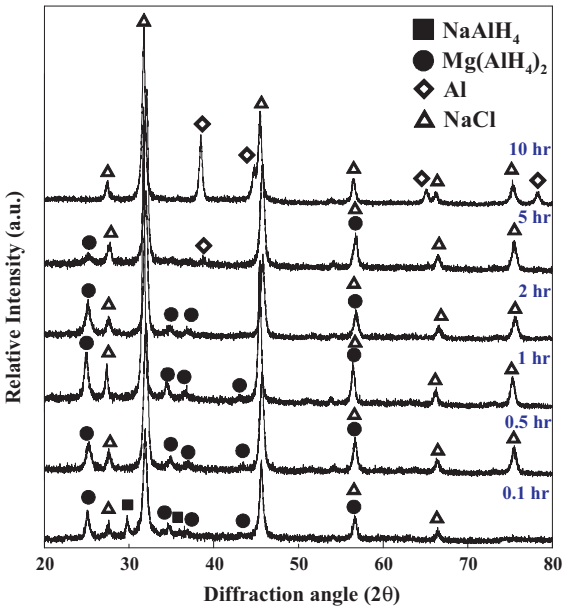

Fig. 1. XRD patterns of the as-synthesized powders milled for 0.1, 0.5, 1, 2, 5 and 10 h.

3. Results and discussion

3.1. Materials characteristics of the synthesized powders

The XRD patterns of the as-synthesized powders prepared with different milling time are shown in Fig. 1. As depicted in this figure, the peaks of $Mg(AlH_4)_2$ and NaCl were found in all synthesized powders, indicating MCAS via reaction (3) mentioned above was effective for $Mg(AlH_4)_2$ fabrication. For the powder prepared with a milling time of 0.1 h, the peaks corresponding to $NaAlH_4$ appeared in the XRD pattern, implying the incomplete metathesis reaction. Prolonging milling time to 0.5–2 h, the absence of the diffraction peaks of the reactants indicated metathesis reaction was completed. However, it was noted that the diffraction peaks of Al appeared in the XRD pattern and even increased in intensity with the milling time over 5 h. Moreover, the absence of the $Mg(AlH_4)_2$ peaks with a 10-h milling indicated that complete dehydrogenation occurred during the prolonged milling process. Based on the XRD results, the synthesized powders could be classified into three categories with different constituents, namely, (1) the hypo-synthesized powder (short milling time) composed of residual $NaAlH_4$, synthesized $Mg(AlH_4)_2$ and NaCl, (2) the complete-synthesized powder (proper milling time) composed of $Mg(AlH_4)_2$ and NaCl, and (3) the hyper-synthesized powder (over milling time) contained various amount of Al and NaCl.

Over-milling caused the generation of excessive heat from the fast impact of the steel balls on the powder precursors and the vessel wall, resulting in the increase of temperature above the decomposition temperature of the synthesized $Mg(AlH_4)_2$. Consequently, the premature dehydrogenation of $Mg(AlH_4)_2$ occurred. Similar observation has been reported by Varin et al. [16], who focused on the synthesis conditions in the range of complete- to hyper-synthesized $Mg(AlH_4)_2$ and the corresponding heat flow events during dehydrogenation reaction. In this present study, the dehydrogenation behavior of the hypo-synthesized powder prepared with a shorter milling time was also explored. As will be discussed later, the residual precursors would affect the dehydrogenation performance.

SEM micrographs showing the morphologies of the raw reactant powders, specifically $NaAlH_4$ and $MgCl_2$, are demonstrated in

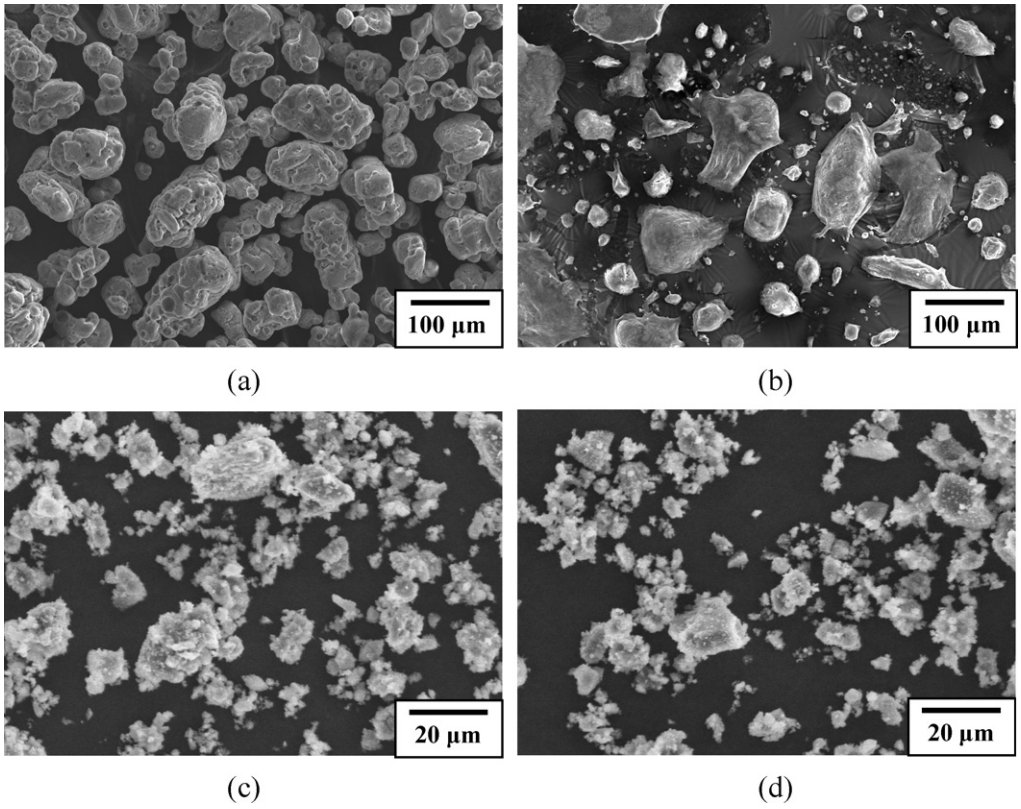

Fig. 2. SEM micrographs of raw reactant powders: (a) $NaAlH_4$, (b) $MgCl_2$ and the various as-synthesized powders milled for (c) 0.5 h, (d) 10 h.

Fig. 2(a) and (b). The particle size of $NaAlH_4$ powder was relatively uniform, while that of flake-shaped $MgCl_2$ powder varied in a wide range from sub-micrometer to hundreds of micrometer. Fig. 2(c) and (d) shows the SEM micrographs of the powders synthesized for 0.5 and 10 h, respectively. The particle size of the synthesized powders was significantly reduced by comparing the SEM micrographs shown in Fig. 2(c) and (d) with those shown in Fig. 2(a) and (b). Extended milling from 0.5 to 10 h, however, did not cause further reduction in particle size as demonstrated in Fig. 2(d). Fig. 3 shows the elements distribution of 0.5 h-synthesized powder, examined by EDS analysis. The distribution of the main elements including Mg, Na, Al and Cl was uniform according to the EDS mapping results shown in Fig. 3. The detection of O indicated that oxidation on the surface of the active $Mg(AlH_4)_2$ was inevitable during MCAS.

3.2. Thermal decomposition and dehydrogenation behavior

Thermal decomposition behavior of various synthesized powders was explored by conducting DTA analysis. The results demonstrated in Fig. 4 were obtained by heating the powders from room temperature to 350 °C at a ramping rate of 5 °C min^{-1} in an argon gas flow of 70 ml min^{-1}. For the MCAS powders prepared with a milling time less than 2 h, two endothermic peaks in the temperature range of 160–180 °C and 250–265 °C, respectively, appeared in each DTA curve. These two endothermic peaks corresponded to the two dehydrogenation reactions. For the 5, 10 h-synthesized powders, however, no peaks were seen in the DTA curves. In these two powders, prolonged milling caused over-synthesis, resulting in the premature dehydrogenation as evidenced in the XRD patterns shown in Fig. 1.

Quantitative evaluation in determining the amount of H_2 desorption and the dehydrogenation temperature of the synthesized powders was performed by thermogravimetric analysis. For the synthesized powders prepared by MCAS with various milling time, the variation of weight change with temperature (from room temperature to 350 °C) for each powder is demonstrated in Fig. 5. As shown in this figure, the shorter the milling time was, the more H_2 was released from the synthesized powder. The temperature at which the synthesized powders started to dehydrogenate also depended on the period of milling time. As shown in Fig. 5, the dehydrogenation commenced at about 100 °C for the 0.1 h-synthesized powder, while that for the 0.5, 1, 2 h-synthesized powders was about 170 °C. The dehydrogenation reaction was almost not visible for the 10 h-synthesized powder. The result for as-received $NaAlH_4$ was also included in this figure for comparison. It was found that $NaAlH_4$ started to dehydrogenate at about 210 °C, which was higher than that of the synthesized $Mg(AlH_4)_2$.

It was noticed that the precursors did not completely reacted under the short milling time such as 0.1 h. As a result, the hypo-synthesized powder still contained some residual $NaAlH_4$ as revealed in the XRD pattern shown in Fig. 1. The lower dehydrogenation temperature observed for the 0.1 h-synthesized powder, as revealed in Fig. 5, suggested that $NaAlH_4$ could destabilize $Mg(AlH_4)_2$ and activate its decomposition at much lower temperature. Srivastava et al. [21] had explored the synergistic effect of $Mg(AlH_4)_2$ on accelerating the dehydrogenation kinetics and lowering the dehydrogenation temperature of $NaAlH_4$. In our case, however, the residual $NaAlH_4$ acted as a promoter for the decomposition of $Mg(AlH_4)_2$. Further investigation on the synergistic behavior of dehydrogenation reaction of $Mg(AlH_4)_2$ and $NaAlH_4$ mixed hydride system was performed with the assistance of in situ synchrotron XRD analysis, as will be discussed later.

The total amounts of H_2 released, based on TGA analysis (Fig. 5), were 3.1 wt%, 2.75 wt%, 2.45 wt%, 2.45 wt% and 0.92 wt% from the powders synthesized by milling for 0.1, 0.5, 1, 2 and 5 h, respectively. The weight change results definitely indicated that the

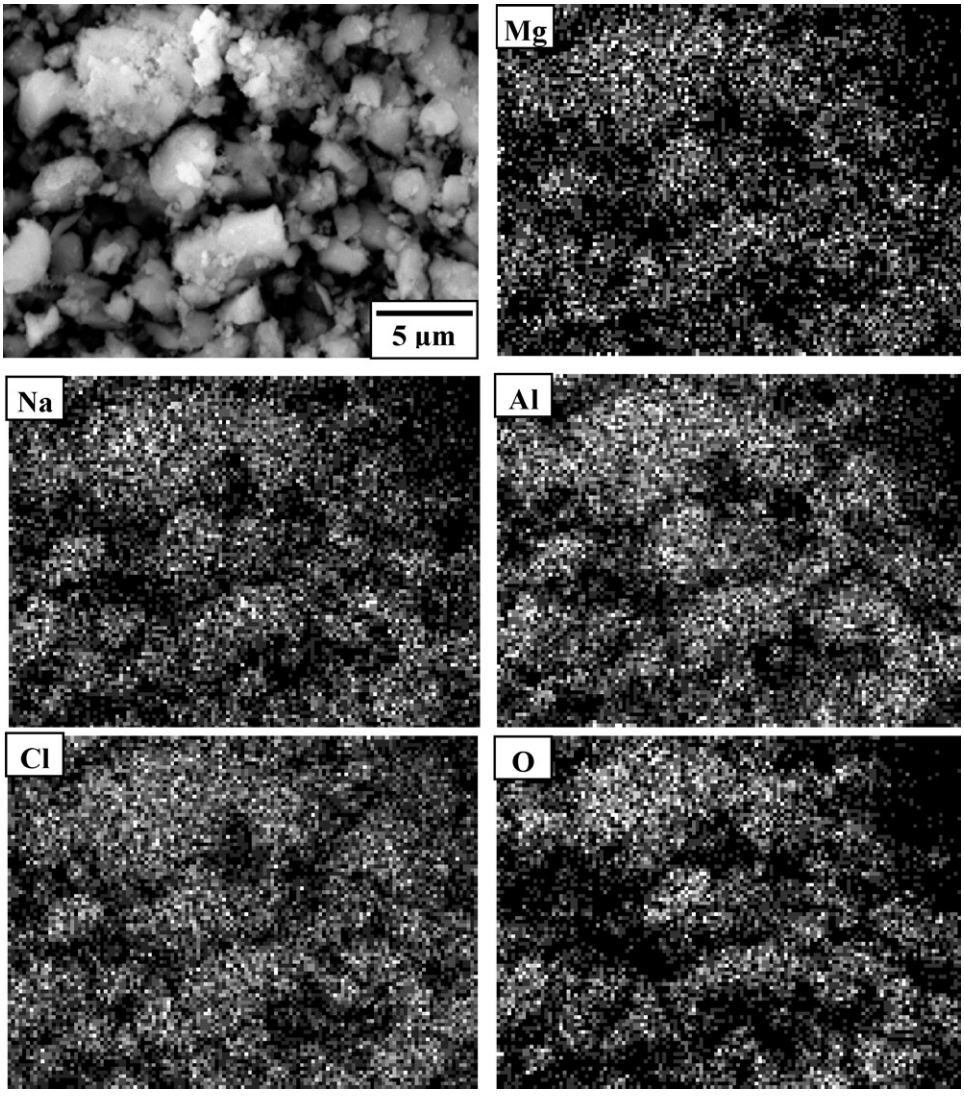

Fig. 3. EDS mappings showing the distributions of Mg, Na, Al, Cl and O in 0.5 h-synthesized powder.

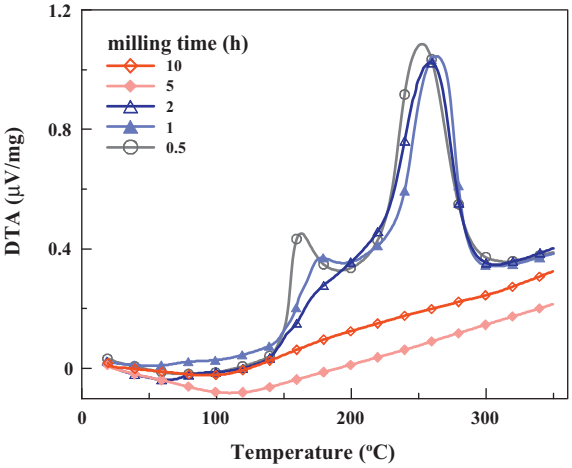

Fig. 4. DTA of the as-synthesized powders milled for 0.5, 1, 2, 5 and 10 h heated from room temperature to 350 °C (ramping rate: 5 °C min^{-1}) in an argon gas flow of 70 ml min^{-1}.

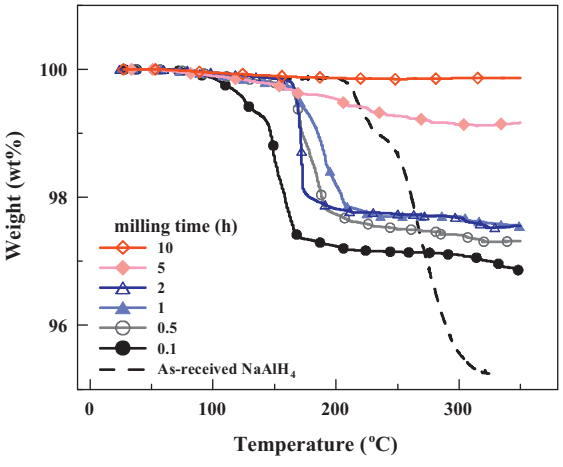

Fig. 5. Thermogravimetric analyses of $NaAlH_4$ and the as-synthesized powders milled for 0.1, 0.5, 1, 2, 5 and 10 h heated from room temperature to 350 °C (ramping rate: 5 °C min^{-1}) under ambient H_2 gas.

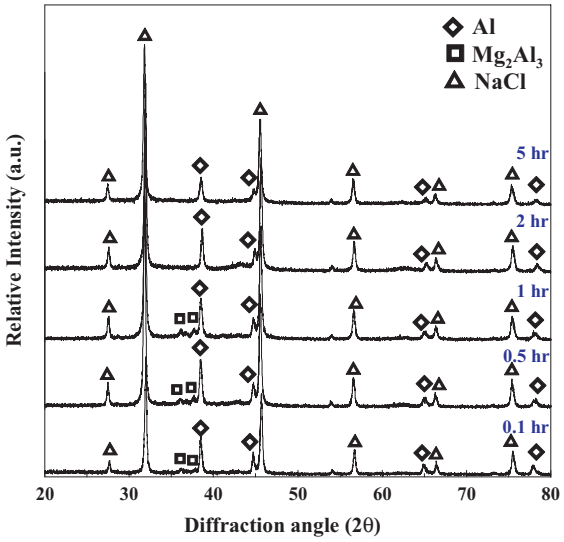

Fig. 6. XRD patterns of the as-synthesized powders milled for 0.1, 0.5, 1, 2 and 5 h after thermal dehydrogenation at 350 °C.

powder prepared with shorter milling time could release higher amount of hydrogen. Besides, the amounts of H_2 released from the second step dehydrogenation reaction were very small as compared with that of the first step reaction. As mentioned above, incomplete MCAS process would leave the reactants, such as $NaAlH_4$, in the synthesized powder. Over-synthesis with prolonged milling time would lead to premature H_2 release of the $Mg(AlH_4)_2$ complex metal hydride. Clearly, the difference in the amounts of H_2 released from the synthesized powders, as measured in TGA analysis, was mainly attributed to the final composition of powders after MCAS process. It was also noted that these values were lower than the theoretical capacity of the fully synthesized powders containing $Mg(AlH_4)_2$ and NaCl (3.9 wt%). Even for the complete-synthesized $Mg(AlH_4)_2$ powders milled for 0.5–2 h, the amounts of H_2 release were about 62–70 wt% of the theoretical H_2 density. Beside the incomplete dehydrogenation, oxidation of $Mg(AlH_4)_2$ in the course of MCAS process might be also responsible for the loss of H_2 generation.

The XRD patterns of various synthesized powders after TGA test (up to 350 °C) are shown in Fig. 6. In each pattern, NaCl was identified, which was the main product of MCAS process, other than $Mg(AlH_4)_2$. The diffraction pattern of the 0.1 h-synthesized powder revealed the presences of metallic Al and Mg_2Al_3, which were resulted from the thermal dehydrogenation of $Mg(AlH_4)_2$. In the referred studies on the dehydrogenation of $NaAlH_4$ powder by several other researchers [22–24], Al and NaH had been identified after TGA test. The authors of these investigations concluded that $NaAlH_4$ would decompose to Na_3AlH_6, Al, NaH and gaseous H_2 during heating to 350 °C. However, none of these species were identified in the XRD patterns shown in Fig. 6. For the 0.5 and 1 h-synthesized powders, the diffraction patterns showed that the dehydrogenated powders consisted of Al and intermetallic Mg_2Al_3 alloy. The presence of Mg_2Al_3 was also originated from the dehydrogenation reaction. In the diffraction patterns of the 2 and 5 h-synthesized powders, only Al peaks, beside those of NaCl, were observed after TGA test. The absence of the peaks of $Mg(AlH_4)_2$ in each XRD pattern indicated that complete dehydrogenation occurred after heating the powders to 350 °C.

Thermal decomposition behavior of as-received $NaAlH_4$ and MCAS-prepared $Mg(AlH_4)_2$ was studied by in situ synchrotron X-ray diffraction, respectively. During in situ synchrotron X-ray diffraction analysis, the powders were heated at a rate of 5 °C min^{-1} from room temperature up to 365 °C to induce the dehydrogenation reactions. The diffraction patterns were then collected every 10 or 20 °C and compiled to give a result shown in Figs. 7(a), 8(a) and 9(a). For the as-received $NaAlH_4$, as shown in Fig. 7(a), the presence of Na_3AlH_6 peaks accompanied with the decreasing intensity of $NaAlH_4$ peaks was observed at temperature higher than 175 °C. This change was associated with the first step dehydrogenation reaction, namely $NaAlH_4 \rightarrow 1/3Na_3AlH_6 + 2/3Al + H_2$. Continued heating to about 275 °C, the formation of NaH as well as the gradually decreasing intensity of Na_3AlH_6 indicated the onset of the second step dehydrogenation reaction as $1/3Na_3AlH_6 \rightarrow NaH + 1/3Al + 1/2H_2$. At temperature higher than 305 °C, the dehydrogenated species, namely NaH and Al, initially oxidized to form $NaAlO_2$. The progressive transformation of reaction products in view of their relative intensities obtained from in situ XRD analyses are shown in Fig. 7(b). The effect of temperature on dehydrogenation reaction is clearly demonstrated.

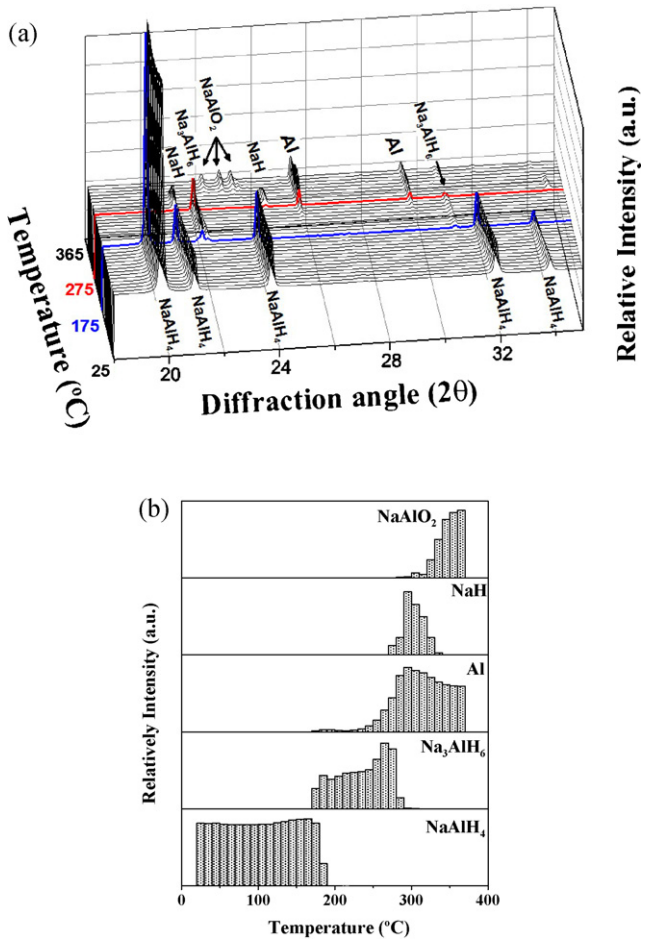

Fig. 7. (a) In situ synchrotron XRD patterns of the as-received $NaAlH_4$ heated from room temperature to 365 °C; and (b) variation of the strongest peak intensity with temperature for the major species appeared during thermal treatment.

The in situ synchrotron XRD patterns of the MCAS powder containing $Mg(AlH_4)_2$, prepared by milling for 0.5 h and heating from room temperature to 365 °C are shown in Fig. 8(a). At temperature below 145 °C, $Mg(AlH_4)_2$ was stable and no significant change was observed. Increasing temperature to 165 °C, the presence of MgH_2 and Al peaks and the decreasing intensity of $Mg(AlH_4)_2$ indicated the occurrence of the first step dehydrogenation reaction, described as $Mg(AlH_4)_2 \rightarrow MgH_2 + 2Al + 3H_2$, basically in agreement with reaction (4) reported by others [12,16–19]. The dependence of the relative intensity on temperature for the major phases

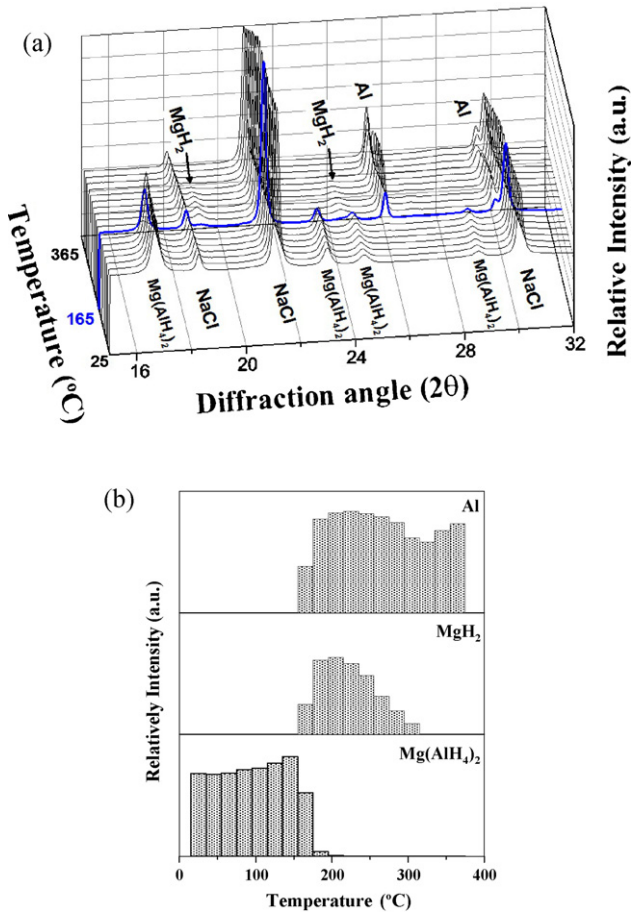

Fig. 8. (a) In situ synchrotron XRD patterns of the 0.5 h-synthesized powder heated from room temperature to 365 °C; and (b) variation of the strongest peak intensity with temperature for the major species appeared during thermal treatment.

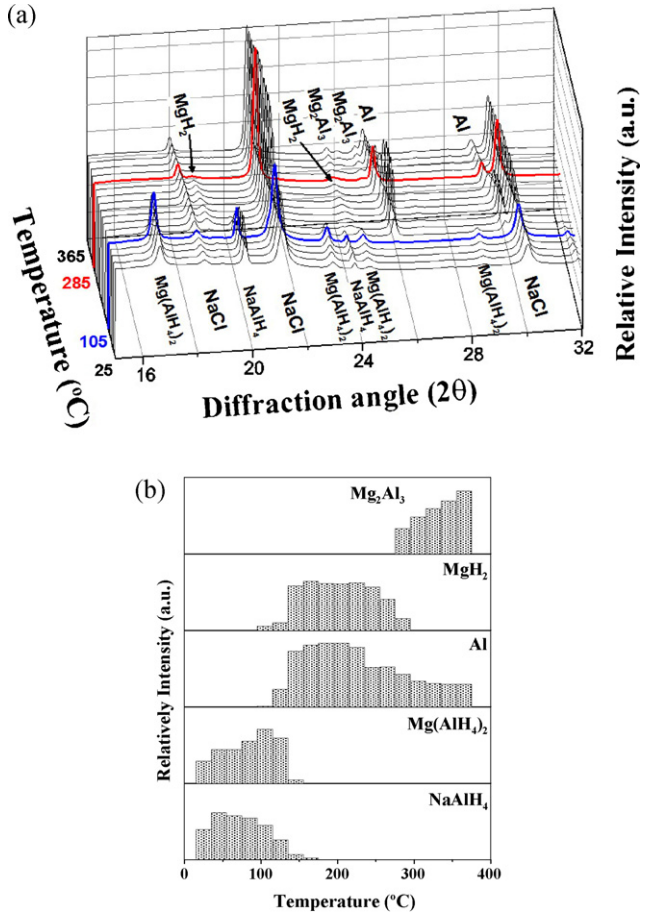

Fig. 9. (a) In situ synchrotron XRD patterns of the 0.1 h-synthesized powder heated from room temperature to 365 °C; and (b) variation of the strongest peak intensity with temperature for the major species appeared during thermal treatment.

is also depicted in Fig. 8(b). At 205 °C, the peaks corresponding to $Mg(AlH_4)_2$ disappeared, indicating the completion of the first step dehydrogenation. The steady peak intensities of MgH_2 and Al also indicated the occurrence of the first step dehydrogenation. Continued heating to the temperature range of 225–305 °C, the peak intensity of MgH_2 gradually reduced, indicating the occurrence of the second step dehydrogenation, mostly described as $MgH_2 + 2Al \rightarrow 0.5Mg_2Al_3 + 0.5Al + H_2$. The absence of Mg_2Al_3 peaks in Fig. 8(a) was due to the small amount of loading used in in situ XRD analysis. However, according to the XRD patterns of 0.5 h-synthesized powder after TGA measurement at 350 °C as revealed in Fig. 6, the reaction of MgH_2 and Al to form Mg_2Al_3 was confirmed. Throughout the whole temperature scanning, NaCl as the by-product of MCAS was identified and remained stable without change.

The in situ synchrotron XRD patterns of the MCAS powder containing $Mg(AlH_4)_2$ and $NaAlH_4$, prepared by milling for 0.1 h and heating from room temperature to 365 °C are shown in Fig. 9(a). Since the 0.1 h-synthesized powder was a mixture consisting of $Mg(AlH_4)_2$, residual $NaAlH_4$ and NaCl, the lower temperature XRD patterns revealed their contribution as shown in Fig. 9(a). Increasing the temperature to 105 °C, no significant change with regard to phase transformation was observed. As the temperature was raised to 125 °C, the peaks associated with Al and MgH_2 began to appear, indicating the initiation of the first step dehydrogenation reaction like that of 0.5 h-synthesized powder. It was likely that the initial dehydrogenation temperature was between 105 and 125 °C when the synthesized powder was heated up. By comparing with that of the completely synthesized powder (with 0.5 h milling time), the initial dehydrogenation temperature was about 60 °C lower with the co-existence of $Mg(AlH_4)_2$ and $NaAlH_4$. The latter seemed to behave as a catalyst for the dehydrogenation of $Mg(AlH_4)_2$.

The variation of the relative intensity with temperature for the major species is demonstrated in Fig. 9(b). The detection of MgH_2 and Al peaks at temperature as low as 105 °C indicated that decomposition of $Mg(AlH_4)_2$ was assisted by the presence of $NaAlH_4$. The absence of $Mg(AlH_4)_2$ peaks at about 165 °C again suggested the completion of the first step dehydrogenation of $Mg(AlH_4)_2$. The fact that the intensity of $NaAlH_4$ peaks started to decrease at temperature below 105 °C, as shown in Fig. 9(b), might also suggest that $Mg(AlH_4)_2$ could assist dehydrogenation of $NaAlH_4$.

Continued heating the 0.1 h-synthesized powder to about 265 °C, the diffraction patterns revealed that Al and MgH_2, beside NaCl, were the main phases present. As the temperature was raised above 285 °C, MgH_2 and Al gradually decreased in their intensities, indicating the occurrence of the second step dehydrogenation via $MgH_2 + 2Al \rightarrow 0.5Mg_2Al_3 + 0.5Al + H_2$ reaction. The presence of Mg_2Al_3 peaks in the diffraction patterns above 285 °C confirmed this reaction. The dehydrogenation behavior of mixed $NaAlH_4$ and $Mg(AlH_4)_2$ powders was different from their single constituent. The synergistic and mutual catalytic effects of them, not only on lowering the initial dehydrogenation temperature of mixed hydrides but also on releasing more amount of H_2 than the individual $Mg(AlH_4)_2$, were noticed. The mutual catalytic effect on both $NaAlH_4$ and $Mg(AlH_4)_2$ in dehydrogenation reaction needs further investigation.

4. Conclusions

$Mg(AlH_4)_2$ was prepared by a MCAS process employing $NaAlH_4$ and $MgCl_2$ as precursors. The synthesis was completed with a milling time controlled at 0.5–2 h. The results of HPTGA analyses showed that the maximum amount about 3.1 wt% of H_2 could be released from the MCAS powder which consisted of $Mg(AlH_4)_2$ and residual $NaAlH_4$. Over milling for a time greater than 2 h caused premature dehydrogenation from the MCAS powders. In situ synchrotron XRD analysis confirmed the two-dehydrogenation reaction of $Mg(AlH_4)_2$. Both HPTGA and in situ XRD analyses showed that the presence of $NaAlH_4$ could assist dehydrogenation of $Mg(AlH_4)_2$ by lowering the initial dehydrogenation temperature close to around 100–105 °C, which was about 60–70 °C lower than that of plain $Mg(AlH_4)_2$ hydride.

Acknowledgement

The authors would like to thank the National Science Council of Republic of China (Taiwan) for financial supports under grant NSC 97-2221-E-006-113-MY3.

References

[1] D. Chandra, J.J. Reilly, R. Chellappa, JOM 58 (2006) 26–32.
[2] S. Orimo, Y. Nakamori, J.R. Eliseo, A. Zuttel, C.M. Jensen, Chem. Rev. 107 (2007) 4111–4132.
[3] B. Sakintuna, F. Lamari-Darkrim, M. Hirscher, Int. J. Hydrogen Energy 32 (2007) 1121–1140.
[4] S. Satyapal, J. Petrovic, C. Read, G. Thomas, G. Ordaz, Catal. Today 120 (2007) 246–256.
[5] W. Grochala, P.P. Edwards, Chem. Rev. 104 (2004) 1283–1315.
[6] J. Larminie, A. Dicks, Fuel Cell Systems Explained, Second ed., John Wiley and sons, Chichester, UK, 2003.
[7] Y. Nakamori, K. Miwa, A. Ninomiya, H.W. Li, N. Ohba, S. Towata, A. Zuttel, S. Orimo, Phys. Rev. B 74 (2006) 045126.
[8] Y. Nakamori, H.W. Li, K. Kikuchi, M. Aoki, K. Miwa, S. Towata, S. Orimo, J. Alloys Compd. 446–447 (446) (2007) 296–300.
[9] Y. Nakamori, H.W. Li, M. Matsuo, K. Miwa, S. Towata, S. Orimo, J. Phys. Chem. Solids 69 (2008) 2292–2296.
[10] E. Wiberg, R. Bauer, Z. Naturforsch. 5 (1950) 396–397.
[11] M. Fichtner, O. Fuhr, J. Alloys Compd. 345 (2002) 286–296.
[12] M. Fichtner, O. Fuhr, O. Kircher, J. Alloys Compd. 356–357 (356) (2003) 418–420.
[13] M. Fichtner, J. Engel, O. Fuhr, A. Gloss, O. Rubner, R. Ahlrichs, Inorg. Chem. 42 (2003) 7060–7066.
[14] K. Komiya, N. Morisaku, Y. Shinzato, K. Ikeda, S. Orimo, Y. Ohki, K. Tatsumi, H. Yukawa, M. Morinaga, J. Alloys Compd. 446–447 (446) (2007) 237–240.
[15] R.A. Varin, Ch. Chiu, T. Czujko, Z. Wronski, Nanotechnology 16 (2005) 2261–2274.
[16] R.A. Varin, Ch. Chiu, T. Czujko, Z. Wronski, J. Alloys Compd. 439 (2007) 302–311.
[17] M. Mamatha, B. Bogdanovic, M. Felderhoff, A. Pommerin, W. Schmidt, F. Schuth, C. Weidenthaler, J. Alloys Compd. 407 (2006) 78–86.
[18] M. Mamatha, C. Weidenthaler, A. Pommerin, M. Felderhoff, F. Schuth, J. Alloys Compd. 416 (2006) 303–314.
[19] Y. Kim, E.K. Lee, J.H. Shim, Y.W. Cho, K.B. Yoon, J. Alloys Compd. 422 (2006) 283–287.
[20] P. Claudy, B. Bonnetot, J.M. Letoffe, J. Therm. Anal. Calorim. 15 (1979) 119–128.
[21] M. Sterlin Leo Hudson, D. Pukazhelvan, G. Irene Sheeja, O.N. Srivastava, Int. J. Hydrogen Energy 32 (2007) 4933–4938.
[22] P. Claudy, B. Bonnetot, G. Chahine, J.M. Letoffe, Thermochim. Acta 38 (1980) 75–88.
[23] K.J. Gross, S. Guthrie, S. Takara, G. Thomas, J. Alloys Compd. 297 (2000) 270–281.
[24] L. Zaluski, A. Zaluska, J.O. Strom-Olsen, J. Alloys Compd. 290 (1999) 71–78.